KECK Geology Consortium
Learning Science Through Research
Published by Keck Geology Consortium
Short Contributions
29th Annual Symposium Volume
23rd April, 2016
ISBN: 1528-7491

GEOCHEMICAL ANALYSIS OF THE TOROK FORMATION MUDSTONES AT SLOPE MOUNTAIN, ALASKA

EVAN LEWIS, Franklin and Marshall College
Research Advisors: Carol de Wet, Stanley Mertzman

INTRODUCTION

This project utilizes X-ray diffraction (XRD) and X-ray fluorescence (XRF) analytics to produce a chemostratigraphic profile of the upper Torok Formation at Slope Mountain, Alaska (Fig. 1, Shimer and McCarthy, this volume). Chemostratigraphic analyses are an effective means of studying changes in sedimentation rate and ocean geochemistry in mudstones, where traditional facies analysis is more difficult due to the lack of identifiable sedimentary structures in fine-grained silt and clay. The goal of the study was to track changing prodelta depositional conditions within the Torok Formation and gain insight into factors that influenced the evolution of the delta system over time.

BACKGROUND

The geologic history of the North Slope foreland basin range begins with the rifting of the Arctic Alaska microplate from the North American continent in the Jurassic (Bird, 1992). The counter clockwise rotation of the plate led to a collision with island arc terranes, leading to the Brooks Range orogeny and formation of the adjacent foreland basin, also known as the Colville Basin (Bird, 1992). The Brooks Range is composed of a series of uplifted thrust sheets that expose belts of varying rock types (Moore et al, 1994). The Barrow Arch antiform separates the North Slope foreland basin from the Canada Basin further north (Bird, 1992). Additionally, the Okhotsk-Chukotka volcanic belt of Eastern Siberia began to deposit thick layers of tuff over Alaska's North Slope at this time (Shimer et al., 2016).

Slope Mountain consists of strata from the Albian-Cenomanian Nanushuk and Torok formations (Fig. 3, Shimer and McCarthy, this volume). The Nanushuk Formation is classified as a succession of intertonguing marine and non-marine units (LePain et al., 2009), while the Torok Formation, from which all samples were collected, is composed of dark grey silty shales, mudstones and clay shales, with interbeds of thinly bedded siltstones and medium to fine grained sandstones deposited in marine slope and basin floor settings in the Torok-Nanushuk depositional wedge (Mull et al., 2003). The Torok Formation ranges in thickness laterally from about 5,600 m to 900 m, though seismic data suggests the formation has been tectonically thickened through complex folding and thrust faulting (Mull et al., 2003). Based on fossil evidence, the strata at Slope Mountain are Aptian to Albian in age, with a limited suite of fossil ammonites and bivalves, as well as foraminifera and palynomorphs at higher elevations (Mull et al., 2003; LePain et al., 2009).

ANALYTICAL METHODS

This study made use of advanced instrumentation in the analytics laboratory at Franklin and Marshall College, including a PANalytical X'Pert Pro X-ray Diffractometer equipped with a ceramic Cu X-ray tube and a PANalytical 2404 X-ray Fluorescence vacuum. For detailed descriptions of the methodology used in this project, see the links listed below.

Crushing

www.fandm.edu/earth-environment/laboratory-facilities/instrument-use-and-instructions/cutting-crushing

XRD Ppreparations Techniques

www.fandm.edu/earth-environment/laboratory-facilities/xrf-and-xrd-lab/x-ray-diffraction

Loss on Ignition (LOI) Preparation Techniques

www.fandm.edu/earth-environment/laboratory-facilities/instrument-use-and-instructions/loi-and-iron-titrations-techniques

XRF Major Element Preparations Techniques

www.fandm.edu/earth-environment/laboratory-facilities/instrument-use-and-instructions/major-element-technique

XRF Trace Element Preparations Techniques

www.fandm.edu/earth-environment/laboratory-facilities/instrument-use-and-instructions/trace-element-technique

Enrichment Factor (EF) Values were calculated with the following equation:

EF element X = (X sample /Al sample) / (X average shale / Al average shale)

For this equation weight percent values are converted to ppm and normalized to aluminum (Al) and standard values of average shale (Tribovillard et al., 2006).

GEOCHEMICAL RESULTS

XRF Data

XRF major and trace element results appear in Table 1. At SM1 major element variations don't fluctuate considerably through the section, except at 25 m, where all major element profiles spike either in a positive or negative direction. SiO_2, TiO_2, Al_2O_3, Na_2O and K_2O abundances decrease at the 25 m elevation while Fe_2O_3, MnO, MgO, CaO and P_2O_5 abundances increase at this elevation (Fig. 1). Similar fluctuations in abundance can be observed at SM2, where SiO_2, TiO_2, Al_2O_3, Na_2O and K_2O abundances decrease at the 32 m elevation mark, and Fe_2O_3, MnO, MgO, CaO and P_2O_5 abundances increase at this elevation (Fig. 1).

Trace element concentrations also show patterns in fluctuating abundance within the SM1 and SM2 stratigraphic profiles. At 32 m in the SM2 profile, Co, Cr, Cu, Ni, V and Zn exhibit negative abundances, relative to other elements (Fig. 1). At this same elevation Ba, Pb, Sr, Th, U and Zr exhibit increases in abundance. At the 25 m mark in the SM1 profile elemental abundances follow similar trends, however, the resolution of data within the profile makes analysis difficult. It appears Ba, Ni, Pb, U, Zn and Zr seem to decrease in their abundance at the 25 m elevation but Co, Sr and Th appear to increase. Some elemental abundances don't fluctuate at all over the SM1 profile. These elements include Cr, Cu and V.

The following observations were made when comparing elemental abundances within SM1 and SM2 profiles to published average shale and crustal abundances worldwide (Fig. 1). In the SM1 section V, Zn, Ni Co and Ba have elemental abundances greater than those observed in typical shales, while U, Cu and Cr abundances are lower than published values (Tribovillard et al, 2006). In the SM2 profile V, Zn, Ni and Co have elemental abundances greater than those documented in typical shales (Fig. 1). U, Cu, Cr and Ba have abundances fluctuating around the standard elemental abundance for shale with the exception of Cr which trends towards being slightly negative.

Enrichment Factors (EF values) were calculated for each major and minor element abundance including; Mn, Ba, Co, Cr, Cu, Ni, U, V, Ni and Zn. These values were calculated and their fluctuations documented throughout SM1 and SM2 stratigraphy. Most elements generally trended towards having neutral enrichment values, though several positive (enrichment) and negative (depletion) excursions do occur at some stratigraphic intervals. Elements, which trended towards having neutral enrichment factors throughout the SM2 profile include Mn, Ba, Cu, and U, while Cr has a depleted EF, and Co, Ni, V and Zn trended towards having enriched EF profiles. Zones of heavy enrichment and depletion were recorded at 14 m and 32 m up-section through SM2. Elements that trended

SM2 (ID)	Si	Ti	Al	Fe	Mg	Ca	Na	K	Ba	Ce	Co	Cr	Cu	Ga	Ni	Pb	Sr	Th	U	V	Y	Zn	Zr
50	*49.5*	*0.6*	*9.0*	*36.8*	*1.1*	*0.1*	*0.4*	*1.4*	570	67	33	70	35	17	69	19	164	34	3	137	47	122	232
46	*65.0*	*1.0*	*17.6*	*7.9*	*2.1*	*0.8*	*1.4*	*2.8*	787	72	35	68	40	20	80	26	123	39	2	134	37	152	242
44	*72.5*	*0.8*	*13.2*	*7.6*	*1.6*	*1.1*	*1.1*	*1.8*	725	75	37	58	59	22	94	30	125	40	1	157	41	166	244
43	*70.2*	*1.0*	*15.5*	*6.9*	*1.9*	*0.8*	*1.0*	*2.4*	642	76	38	48	54	24	84	35	129	46	2	166	39	164	245
40	*68.0*	*0.9*	*16.6*	*7.6*	*2.0*	*0.8*	*1.3*	*2.5*	715	78	35	63	50	25	82	38	140	42	2	174	38	153	258
38	*66.8*	*1.0*	*17.8*	*7.5*	*2.0*	*0.6*	*1.3*	*2.7*	609	71	33	68	46	23	81	32	140	40	3	158	35	147	246
36	*69.2*	*0.9*	*16.0*	*6.5*	*2.2*	*1.0*	*1.5*	*2.4*	586	69	31	64	39	20	73	39	121	37	2	145	36	132	261
34	*72.8*	*0.8*	*14.0*	*6.4*	*1.7*	*0.8*	*1.3*	*2.0*	689	73	32	58	44	19	73	15	135	36	1	145	34	140	233
32.75	*71.3*	*0.8*	*13.3*	*7.4*	*1.9*	*2.2*	*1.0*	*2.0*	6519	-59	0	8	0	0	10	85	714	0	1	31	10	11	56
32.5	*3.8*	*0.0*	*2.5*	*3.2*	*0.6*	*89.1*	*0.2*	*0.1*	2109	99	15	0	19	22	43	89	231	92	9	95	30	116	474
32.25	*52.4*	*0.9*	*36.7*	*3.3*	*1.2*	*2.5*	*0.5*	*2.3*	4455	8	0	9	5	6	24	65	918	0	4	78	8	39	195
32	*22.7*	*0.3*	*16.5*	*4.8*	*0.9*	*53.3*	*0.4*	*0.6*	763	86	29	63	44	23	67	14	165	40	4	150	34	128	254
30	*71.9*	*0.8*	*15.1*	*5.8*	*1.7*	*0.8*	*1.5*	*2.2*	595	73	32	50	45	23	75	34	147	45	3	157	34	138	257
28	*69.7*	*0.9*	*15.8*	*6.3*	*2.1*	*1.0*	*1.6*	*2.4*	854	88	36	52	50	26	85	29	148	43	1	176	37	155	253
26	*69.0*	*0.9*	*16.8*	*6.6*	*1.9*	*0.6*	*1.4*	*2.6*	777	81	34	55	47	23	80	30	148	44	2	161	36	148	247
24	*70.1*	*0.9*	*16.2*	*6.6*	*1.8*	*0.5*	*1.3*	*2.4*	766	75	35	58	48	23	83	34	148	42	2	169	37	148	267
22	*69.6*	*1.0*	*16.6*	*6.5*	*1.8*	*0.4*	*1.4*	*2.4*	649	75	31	71	41	23	78	18	129	39	4	164	33	143	262
20	*70.7*	*0.9*	*16.1*	*6.0*	*1.7*	*0.5*	*1.5*	*2.4*	770	73	38	68	48	21	87	38	144	37	3	155	35	146	234
18(2)	*70.3*	*0.9*	*15.3*	*7.3*	*1.8*	*0.7*	*1.2*	*2.3*	590	62	35	48	45	19	80	21	118	42	2	138	32	141	220
18(1)	*73.8*	*0.8*	*13.2*	*6.4*	*1.7*	*0.8*	*1.1*	*2.0*	663	73	33	57	42	23	77	28	152	41	1	155	35	148	241
16	*69.7*	*0.9*	*16.1*	*6.4*	*2.0*	*0.7*	*1.6*	*2.4*	705	78	40	67	49	22	85	39	128	38	1	151	34	149	230
14(2)	*70.0*	*0.9*	*15.8*	*6.7*	*1.9*	*0.6*	*1.5*	*2.3*	786	76	31	59	41	20	74	36	125	38	1	135	37	145	242
14(1)	*73.0*	*0.8*	*13.8*	*6.1*	*1.7*	*1.1*	*1.2*	*2.0*	-31	122	43	54	64	10	39	11	182	52	0	216	32	99	89
12	*34.7*	*0.7*	*11.8*	*40.6*	*5.0*	*3.5*	*0.7*	*2.2*	723	73	38	50	54	25	88	23	129	45	2	177	36	172	237
10	*67.9*	*1.0*	*17.1*	*7.0*	*2.2*	*0.7*	*1.2*	*2.7*	835	79	37	57	56	23	88	25	144	44	4	175	37	165	261
8(2)	*68.0*	*1.0*	*16.8*	*7.0*	*2.2*	*0.8*	*1.3*	*2.6*	626	77	35	89	36	20	77	33	154	34	3	136	54	150	242
8(1)	*69.8*	*0.8*	*14.3*	*7.2*	*1.7*	*2.2*	*1.2*	*2.1*	101	112	42	54	58	11	36	18	216	47	0	211	32	98	112
6(2)	*35.3*	*0.7*	*12.0*	*37.9*	*4.9*	*5.1*	*0.8*	*2.2*	802	98	40	59	56	23	88	34	156	49	3	167	41	161	388
6(1)	*68.8*	*1.0*	*16.7*	*7.3*	*1.7*	*0.4*	*1.3*	*2.5*	678	74	29	73	37	22	62	44	120	41	2	155	27	111	245
5.4	*72.8*	*0.9*	*14.8*	*6.4*	*1.3*	*0.2*	*1.3*	*2.2*	734	89	22	95	30	19	36	34	133	42	2	161	27	65	243
4	*72.3*	*0.9*	*13.4*	*8.3*	*0.9*	*0.7*	*1.3*	*2.2*	515	71	43	63	37	19	90	33	107	40	1	128	34	163	229
2	*73.4*	*0.8*	*13.4*	*6.3*	*1.6*	*1.0*	*1.3*	*1.9*	661	65	33	62	35	19	79	16	104	37	1	131	34	146	256
1	*75.1*	*0.8*	*13.0*	*5.8*	*1.5*	*0.6*	*1.2*	*1.8*	783	86	37	62	51	24	84	40	113	40	1	171	38	173	228

Table 1. Select trace and major elemental data recorded from geochemical analysis from SM2. Major element abundances (italics) were recorded as normalized weight percentages and trace elemental abundances are recorded in ppm. Values below zero are to be considered out of the detectable range of the analytical equipment.

towards having neutral enrichment factors throughout SM1 include Mn, Cu and U while elements with enriched EF profiles include Ba, Co, Ni, V and Zn and only Cr has a depleted value.

LOI Data

Loss on ignition (LOI) was calculated for each SM1 and SM2 sample. The highest LOI value recorded throughout the stratigraphy was calculated to be 3.4%, while the smallest recorded LOI value was determined to be 0.2%. Over the range of the SM1 profile, LOI fluctuates across the 0.4% boundary and there is a significant increase at the 25m elevation with a recorded LOI of about 2%. The SM2 samples have a broader range of LOI variation. Calculated LOI values in the SM2 profile fluctuate across the 0.5% mark and periodically increase to LOI values between 1.5% and 2%, with one large increase at 32 m where LOI reaches 3.5%.

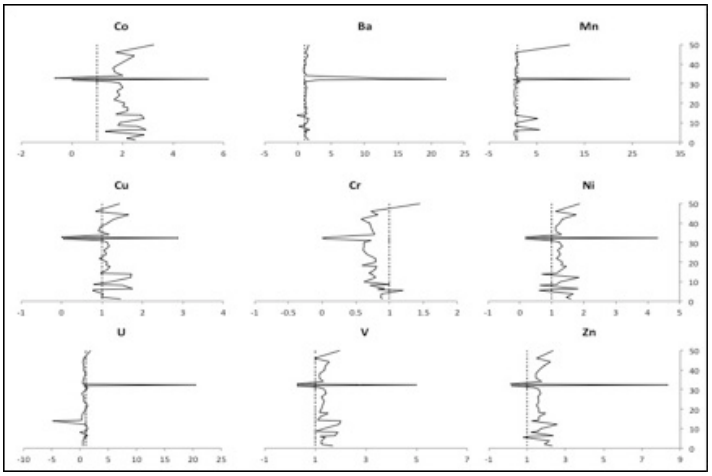

Figure 1. These figures plot select trace element enrichment factor (EF) values (solid line) at SM2 against stratigraphic elevation. The dotted line represents average abundance of trace element in marine shales.

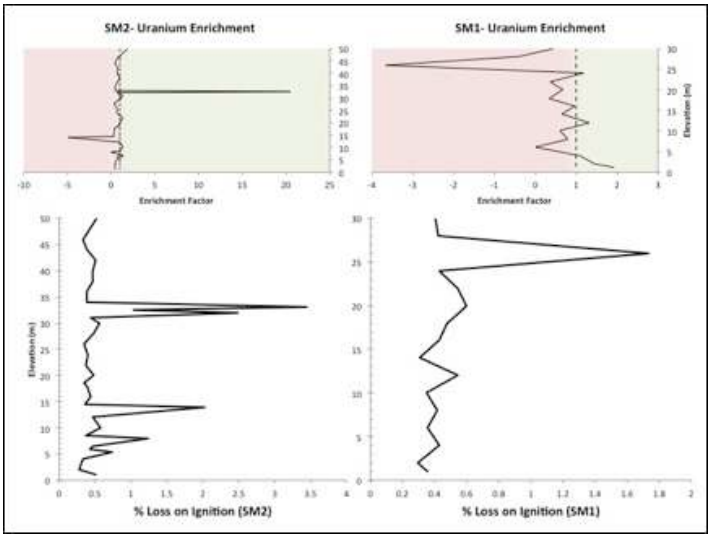

Figure 2. This figure displays comparative U enrichment factor (EF) values and LOI chemostratigraphic profiles for SM1 and SM2. Positive and negative correlations can be observed between both sections in LOI and U EF elevations of 14m (SM2) and 26m (SM1).

DISCUSSION

Correlation

Based on field observations we estimated the base sample in SM1 was correlative with an approximate elevation of 30 m in SM2. Geochemical results roughly support these field observations. LOI and U enrichment profiles within the two sections have similar trends at elevations near those observed in the field. LOI fluctuations rarely deviate more than 0.1% from the background values, except where 2 increases in LOI values (1.7% and 2.0% respectively) occur in both SM1 and SM2. These LOI peaks correlate between SM1-26 and SM2-14 (Fig. 2).

Enrichment factor profiles as discussed above, provide additional evidence of this correlation. Significant increases in Uranium EF values occur at similar elevations. Uranium EF values of -4.8 and -3.8 are recorded at elevations of 14 m in SM2 and 26 m in SM1 respectively (Fig. 2). These two lines of evidence provide a strong argument for the SM1 and SM2 sections being correlative between elevations of SM1-26 and SM1-14. Despite the likely correlative relationship between SM1 and SM2, we did not combine the datasets for the analyses of SM2 described below.

Anomalous Layer

The most dramatic feature of the EF diagrams is an anomalous layer at 32.5 m in SM2 (Fig. 1). At 32.5 m minor elements spike in enrichment, with the exception of chromium (Cr), which dropped to below the background value. The relative decrease in abundance of chromium at this elevation can be explained several ways. Chromium concentrations are strongly influenced by detrital deposition, but chromium (which is soluble in normal oxygenated water) is typically enriched in anoxic environments (Tribovillard et al, 2006). Therefore, the abrupt decrease in the Cr EF values could be explained by a rapid change in ocean chemistry to a more oxidizing state. Additional evidence, however, indicates the 32.5 m horizon may have been altered post-deposition. Thin layers of barium (Ba)-enriched calcite and barite ($BaSO_4$) were observed confining the 32.5 horizon. These confining layers of calcite appear to have slickenlines typical of fracture fill. Barium is typically enriched in hydrothermally altered environments, suggesting the confining layers are probably associated with hydrothermal mineralization as a result of low angle faulting or fracturing. The low levels of Cr in the 32.5 horizon are likely the result of dissolution via the saturation of hydrothermally heated, Ba-enriched, water permeating throughout the fault zone.

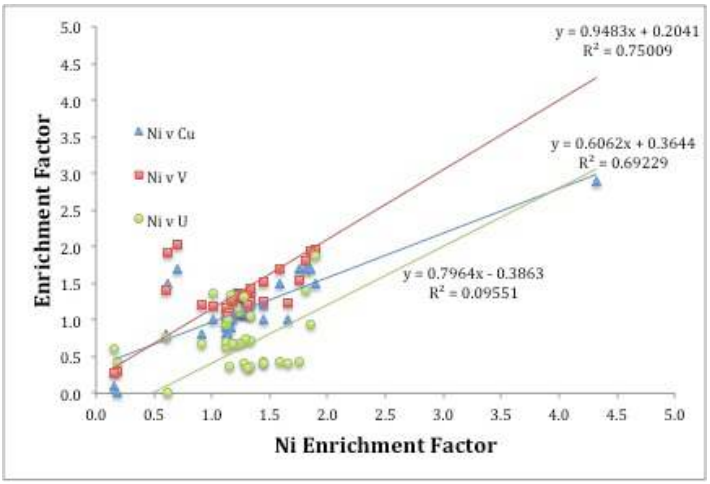

Figure 3. A cross-plot of Cu, V and U enrichment factor (EF) values with Ni illustrates that Cu , V and U are enriched at roughly equal rates to Ni enrichment in the Torok Formation. Slopes and R2 values have been calculated for each linear trend and can be observed above. The positive correlations are used to establish sub-oxic condtions in the Torok Formation.

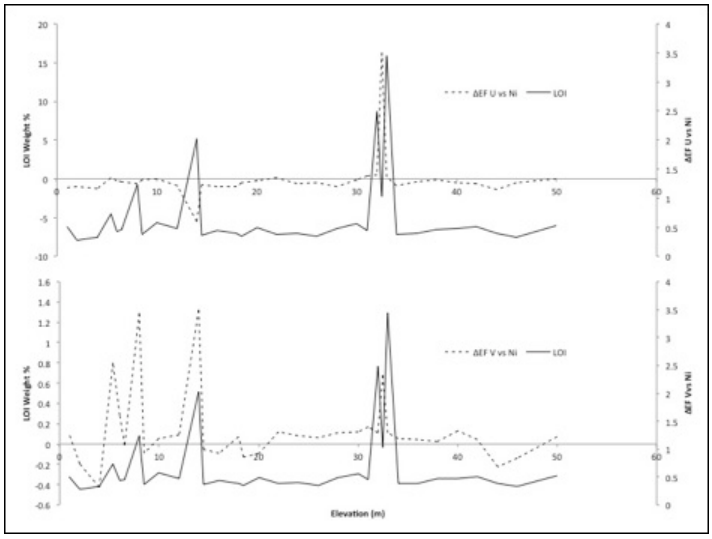

Figure 4. The difference in enrichment factors of U and V plotted against LOI and elevation to display the correlations between Δ EF and LOI. Peaks in LOI generally correlate with peaks in Δ EF of V or U respectively.

Environmental Interpretations

Various trace elements in shales can be used as indicators of oceanic conditions, including paleo-redox and bio-productivity (Tribovillard et al., 2006). Uranium and vanadium are thought to represent reliable paleo-redox proxies while nickel, copper and TOC are typically used as proxies for bio-productivity (Śliwiński et al, 2011). Accumulation of uranium is typically limited in ocean environments due to its unreactive nature, but both uranium and vanadium can become enriched in anoxic bottom waters due to biogenic complexation (Calvert, 1993). This behavior is opposite nickel, copper, and a suite of other minor elements (Tribovillard et al., 2006). Therefore, by comparing EF trends we can better characterize oxygen levels in their depositional regimes.

In oxic-suboxic depositional environments, relative rates of accumulation between uranium/vanadium and nickel/copper are expected to be low and equal to each other (Tribovillard et al, 2006). As the subaqueous depositional environment becomes more anoxic, uranium and vanadium typically become enriched and accumulate at a faster rate than nickel and copper (Tribovillard et al, 2006). This trend continues as the depositional environment becomes euxinic, and the disparity between the two accumulation rates increases further. By comparing enrichment factors between elements we can compare how our samples' rates of enrichment compare with each other as a factor of ocean water Eh. When uranium and vanadium enrichment values are cross-plotted with nickel enrichment values, the linear trends have slopes of 0.79 and 0.94 and R^2 values of 0.09 and 0.74 respectively (Fig. 3). Similarly, enrichment factors for nickel were compared with the enrichment factor of another element enriched in sulfate-reducing conditions, copper. These cross plots comparing nickel vs copper have slopes of 0.6 and R^2 values of 0.68. Because nickel and copper rates of enrichment have positive slopes and strong correlations, it can be inferred the two trace elements accumulated at similar rates at similar times (possibly due to influx of organic material). Nickel and copper accumulation rates in the Torok Formation were behaving as would be expected from models, ie: being enriched at similar rates. It can also be inferred from these cross plots that uranium and vanadium enrichment rates increased linearly with nickel enrichment rates. This suggests both uranium and vanadium accumulated at similar rates to nickel, which is typically indicative of an oxic-suboxic depositional environment.

Δ EF of Metals and Total Organic Carbon

In this analysis Δ EF represents the differences in trace metal abundances relative to each other. Total organic

carbon (TOC) is typically enriched in depositional regimes with anoxic bottom waters (Wright et al, 2010). It is expected that as TOC increases, so will the relative difference in EF values between uranium/vanadium and nickel/copper (Tribovillard et al, 2006). Though we did not calculate TOC in this study, LOI was used as a proxy value, which appears to be an accurate representation due to the very low values calculated for LOI. When comparing the differences between enrichment factors calculated for vanadium and nickel, it can be observed, most spikes in LOI correlates with a large spike in the Δ enrichment of vanadium and nickel (Fig. 4). Similar trends in Δ EF can be observed when looking at enrichment factor trends calculated for uranium and nickel (Fig. 4).

When Δ EF of uranium and nickel is plotted with LOI results, the 32.5 layer shows a drastic increase in both LOI and Δ EF, with that said, at an elevation of 14 m this relationship is reversed (Fig. 4). Correlation between Δ EF and LOI can often be attributed to an increase in organic material into the depositional environment (Tribovillard et al, 2006). Similarly, enrichment of nickel and copper appear to correlate well with LOI data, increasing and decreasing at similar elevations. Together, this suggests in most cases minor element enrichment can be correlated with LOI. Little to no variation between trace elemental abundance/enrichment and TOC is typical of oxic-suboxic depositional environments whereas in anoxic depositional regimes, correlation is possible because minor element enrichment is limited by the availability of organic substrates in the environment (Tribovillard et al, 2006). These conclusions are based on models that use high percentages LOI. For the samples found within SM2, LOI was typically less than 1 weight percent which could account for some discrepancies within the data.

ENVIRONMENTAL CONCLUSIONS

This study demonstrates there is significant promise in the use of chemostratigraphy to identify environmental conditions in the Torok Formation. Though at 2 m intervals the sample resolution is too low for a detailed analysis of fluctuating environmental conditions, broad trends are observable in the major and trace element results. The results suggest the majority of samples taken within the Torok Formation at SM2 were deposited in an oxic-suboxic depositional environment. Further work on the geochemistry of the proximal Torok Formation using these methods may allow for identification of cryptic flooding surfaces that are correlative with unconformities in the Nanushuk Formation. Chemostratigraphy may also be used for correlation over several kilometers of lateral distance, as illustrated by the similar results from SM1 and SM2. In this way we can use the geochemical study of mudstones to enhance our understanding of the Cretaceous depositional regimes.

REFERENCES

Bird, K. J., and Molenaar, C.M., 1992, The North Slope foreland basin, Alaska, in R.W. Macqueen and D.A. Leckie, eds., Foreland fold and thrust belts: AAPG Memoir 55, p. 363-93.

Calvert, S. E., and Pederson, T.F., 1993, Geochemistry of Recent Oxic and Anoxic Marine Sediments: Implications for the Geological Record: Marine Geology, v. 113, p. 67-88.

Houseknecht, D. W., and Schenk, C.J., 2004, Sedimentology and Sequence Stratigraphy of the Cretaceous Nanushuk, Seabee, and Tuluvak Formations Exposed on Umiat Mountain, North-Central Alaska: United States Geological Survey in Alaska 1709, 18 p.

LePain, D. L., McCarthy, P.J., and Kirkham, R., 2009, Sedimentology, Stacking patterns, and Depositional Systems in the Middle Albian, Cenomanian Nanushuk Formation in Outcrop, Central North Slope, Alaska: State of Alaska, Department of Natural Resources, Division of Geological and Geophysical Surveys, 78 p.

Moore, T. E., Wallace, W.K., Bird, K.J, Karl, S.M., Mull, C.G., and Dillon, J.T., 1994, Geology of northern Alaska, in G. Plafker and H.C. Berg, eds., The geology of Alaska: The Geological Society of America, The Geology of North America v. G.1, p. 49-92.

Mull, C.G, Houseknecht, D.W., and Bird, K.J., 2003, Revised Cretaceous and Tertiary Stratigraphic Nomenclature in the Colville Basin, Northern Alaska: U.S. Geological Survey Professional Paper 173, 51 p.

Shimer, G. T., Benowitz, J.A., Layer, P.W., McCarthy, P.J., Hanks, C.L., and Wartes,

M., 2016, 40Ar/39Ar ages and geochemical characterization of Cretaceous bentonites in the Nanushuk, Seabee, Tuluvak, and Schrader Bluff formations, North Slope, Alaska: Cretaceous Research, v. 57, p. 325-41.

Śliwiński, M.G., Whalen, M.T., Newberry, R.J., Payne, J.H., and Day, J.E., 2011, Stable Isotope (δ13Ccarb & org, δ15Norg) and Trace Element Anomalies during the Late Devonian 'punctata Event' in the Western Canada Sedimentary Basin: Palaeogeography, Palaeoclimatology, Palaeoecology, v. 307, p. 245-271.

Tribovillard, N., Algeo, T.J., Lyons, T., and Riboulleau, A., 2006, Trace metals as paleoredox and paleoproductivity proxies: an update: Chemical Geology,v. 232, p. 12-32.

Wright, A. M, et al, 2010, Application of Inorganic Whole Rock Geochemistry to Shale Resource Plays: Canadian Society for Unconventional Gas, 18 p.